Solid State Science and Technology, Vol. 11, No.1 (2003) 25-33

STUDIES ON COLOSSAL MAGNETORESISTANCE $La_{1-x}Ca_xMnO_3$ (x = 0.25, 0.33 AND 0.45) BY ULTRASOUND METHOD

Nor Azah Nik Jaafar, R. Abd-Shukor
School of Applied Physics
Universiti Kebangsaan Malaysia
43600 Bangi, Selangor, Malaysia

ABSTRACT

$La_{1-x}Ca_xMnO_3$ which exhibits colossal magnetoresistance (CMR) effect for x = 0.25, 0.33 and 0.45, was subjected to ultrasound investigations. For all samples, temperature-dependent electrical resistivity measurements showed a metal-insulator transition identified by a peak in resistivity, typical transport behaviour of a CMR material. The x = 0.25 sample showed the highest T_{IM} at 260 K, x = 0.33 at 240 K and x = 0.45 at 150 K. For x = 0.45 sample, a large resistivity hysteresis occurs between 90 to 190 K. Temperature-dependent sound velocity measurements (80 to 300 K) showed a large change in longitudinal velocity of ~6 % takes place just below T_{IM} (insulator-metal transition) for x = 0.25 and 0.33 samples. The sudden increase in Δv was also observed in shear mode for both samples. These frequency hardenings which take place below T_c, indicate the prominent role of lattice vibrations on the physical properties of this material. A characteristic behaviour of ultrasonic attenuation, which decrease sharply in the region below T_c, accompanied the anomalous phonon hardenings. These features, which are closely related with the mechanisme at T_c, have been previously predicted from theoretical calculations based on the combined double-exchange and lattice polaron model. Elastic measurements for x = 0.45 sample showed a completely different behaviour compared to the x = 0.25 and 0.33 samples. This sample showed the largest Δv for both modes within 80 to 210 K measurement range (>10 %). Large thermal hysteresis between 130 to 190 K observed in both shear and longitudinal velocity measurements, were attributed to simultaneous occurrence of conducting ferromagnetic state and charge-ordered state.

INTRODUCTION

Colossal magnetoresistance (CMR) material, which exhibits a large decrease in electrical resistivity under application of a magnetic field has attracted wide interest due to its potential technological application and the need for better theoretical understanding. The CMR effect is associated with paramagnetic-insulating to ferromagnetic-metallic transition at the transition temperature T_c.

This effect, observed in doped manganese oxides, $Ln_{1-x}A_xMnO_3$ (Ln = La, Nd, Pr; A = Sr, Ba, Ca, Pb) was originally attributed to double exchange mechanism [1]. According to this model, conduction occurs via a coherent hopping of electrons between neighboring Mn^{3+} and Mn^{4+} ions. Strong Hund's rule coupling $J_H \gg t$ (t = hopping matrix element) of the electronically active e_g electrons to the localized electrons in t_{2g} orbitals means the motion of electron spin polarizes the localized Mn spins, leading to ferromagnetism. This explains the correlation between ferromagnetism and metallicity.

It was first argued by Millis et al. [2] that double exchange (DE) alone does not suffice to quantitatively explain the metal-insulator transition such as the higher predicted T_c, very high resistivity at $T > T_c$ and the sharp drop of resistivity just below T_c. Millis et al. proposed that dynamic Jahn-Teller polaron due to splitting of Mn e_g states together with the double-exchange effect, make up the physics of the manganates that is responsible for the CMR effect [2-4]. This was followed by many theoretical studies based on the combined model in order to derive the right temperature-dependent resistivity and MR effects.

Theoretical calculations performed using various approaches e.g. mean-field approximation, Monte Carlo stimulation, Kubo formula [5-8], which included the electron-phonon effect, produced results that give a good agreement with experimental data. More importantly, Unjong et al. [6], have shown theoretically that the existing DE model with incorporated small polaron can be improved by taking into account the effects of phonon frequency hardening below T_c. This implies that lattice vibration may play an important role in the properties of these manganates and should be further investigated.

There have been direct experimental evidences on the important role of lattice vibration, for example the large oxygen isotope shift effect [9] and the formation of polarons as evidenced from pair distribution function (PDF) analysis [10] and electron paramagnetic resonance (EPR) signal [11].

The lattice degrees of freedom need to be understood in this material. This includes shifts in phonon frequency as observed by Kim et al. [12], sound velocity anomalies [13,14] and abrupt changes in lattice degrees of freedom [15] at T_c. These results assert the substantial role of phonon in the mechanisms of CMR.

To further shed light on this matter, sound velocity and ultrasonic attenuation [5] measurements are needed to investigate further the relation between T_c and lattice vibration. In this work, ultrasonic investigations were performed on $La_{1-x}Ca_xMnO_3$ (x = 0.25, 0.33, 0.45) which exhibits CMR effect in the range of $0.2 < x < 0.5$.

EXPERIMENTAL DETAILS

$La_{1-x}Ca_xMnO_3$ samples with x = 0.25, 0.33 and 0.45 were prepared using solid-state reaction method. Stoichiometric proportions of La_2O_3, $CaCO_3$ and MnO_2 (purity ≥99.9 %) are mixed and ground thoroughly, and calcined in air at 1150 °C for 24 hrs with intermediate grinding. The resultant powders were pressed into pellets of ~13 mm diameter and ~2 mm thickness. These pellets were sintered in air at 1200 °C for 10 hrs and slow-cooled to room-temperature at a rate of 3 °C/min.

The samples were analyzed by X-ray diffraction technique (XRD) with CuK_α radiation (λ = 1.5418 Å) using a Siemens D 5000 diffractometer. Their microstructural properties were studied using Philips XL 30 scanning electron microscope (SEM). Temperature-dependent electrical resistivity was measured using the dc four-point probe method. To perform the ultrasonic measurements, the pulse-echo overlap method was employed utilising a Matec Model 7700-based system. X-cut and Y-cut quartz transducers were used to generate longitudinal and shear waves respectively at 10 MHz. The sample was bonded to the transducer using Nonaq stopcock grease. Temperature-dependent sound velocity and ultrasonic attenuation measurements were performed in the temperature range of 80 to 300 K with cooling and warming rate at 1 K/min.

RESULTS AND DISCUSSION

All samples showed an orthorhombic symmetry with space group pbnm similar as reported in [16]. The X-ray diffraction patterns of the samples show that they are of single phase structure.

Temperature-dependent electrical resistivity measurements (Fig 1) showed the insulator to metal transition (T_{IM}), a feature that corresponds to CMR properties. The x = 0.25 sample showed T_{IM} at 260 K, x = 0.33 at 240 K and x = 0.45 at 150 K. The x = 0.25 sample showed a sharp resistivity peak, while the x = 0.33 showed a broader transition from insulating to metallic phase with the fall-off in resistivity occured in a larger

temperature range. For $x = 0.45$ sample, a large resistivity hysteresis was observed during cooling and warming.

FIGURE 1 : Resistivity versus temperature curves for $La_{1-x}Ca_xMnO_3$ with $x = 0.25$, 0.33, and 0.45

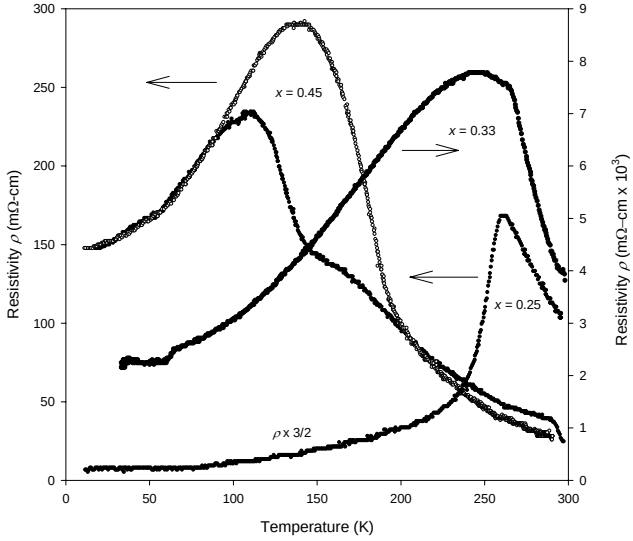

TABLE 1 : Electrical resistivity (at 300 K) and lattice parameters of $La_{1-x}Ca_xMnO_3$ with $x = 0.25$, 0.33 and 0.45.

Sample x	Resistivity $\rho_{300\,K}$ (mΩ cm)	Lattice parameters a (Å)	b (Å)	c(Å)	Lattice volume V(Å^3)
0.25	43	5.472	5.477	7.737	231.9
0.33	1747	5.444	5.466	7.662	228.0
0.45	16	5.410	5.423	7.652	224.5

Table 1 shows the lattice parameters and room temperature electrical resistivity ($\rho_{300\,K}$). The $x = 0.33$ sample has the highest $\rho_{300\,K}$, followed by $x = 0.25$ with $x = 0.45$ has the lowest $\rho_{300\,K}$. The high resistivity observed in $x = 0.33$ sample could be due to the grain size of the sample. SEM micrograph of $x = 0.33$ sample showed a densely packed structure with few voids and pores. There exists a big difference in the degree of porosity between all the three samples with $x = 0.33$ clearly showed fewer voids and pores. From the SEM micrographs, we suggested that the grain size of the $x = 0.33$ is much smaller than that of $x = 0.25$ with $x = 0.45$, the largest grain size. The grain-size effect is made

based on previous report that there is a large discrepancies among the resistivity data of $La_{2/3}Ca_{1/3}MnO_3$ and that there is a close relationship between resistivity and microstructure where the resistivity increased as the grain size decreased [17]. The intragrain resistivity is found to be lower than the intergrain resistivity.

TABLE 2: Mass density, longitudinal velocity (v_l), shear velocity (v_s), transition temperature (T_{IM}), longitudinal modulus (C_L), shear modulus (μ), bulk modulus (B), Young's modulus (E) and Debye temperature (θ_D) of $La_{1-x}Ca_xMnO_3$ for x = 0.25, 0.33, 0.45 in the void-free approximation. (Numbers in parenthesis are measured values)

Sample	x = 0.25	x = 0.33	x = 0.45
Density (g cm^{-3})	5.27 ± 0.03	5.32 ± 0.03	4.31 ± 0.03
Porosity (%)	15.1 ± 0.5	12.2 ± 0.6	26.1 ± 0.4
v_l (km s^{-1})	5.90 ± 0.02	7.03 ± 0.03	6.66 ± 0.02
	(5.06 ± 0.02)	(6.12 ± 0.03)	(5.30 ± 0.02)
v_s (km s^{-1})	3.34 ± 0.01	3.40 ± 0.01	3.38 ± 0.01
	(2.95 ± 0.01)	(3.05 ± 0.01)	(2.77 ± 0.01)
C_L (GPa)	217 ± 2	299 ± 3	259 ± 2
	(135 ± 2)	(200 ± 3)	(121 ± 2)
μ (GPa)	69.4 ± 0.4	69.9 ± 0.4	66.5 ± 0.4
	(45.8 ± 0.6)	(49.5 ± 0.6)	(33.0 ± 0.4)
B (GPa)	124 ± 2	206 ± 3	170 ± 2
	(73.6 ± 2.7)	(134 ± 4)	(76.9 ± 2.2)
E (GPa)	176 ± 7	188 ± 7	177 ± 5
	(114 ± 9)	(132 ± 9)	(86.7 ± 5.9)
T_{IM} (K)	260	240	150
θ_D (K)	542 ± 5	555 ± 6	546 ± 5
	(477 ± 5)	(497 ± 6)	(447 ± 5)

The ultrasonic velocity and attenuation measurements are shown in Fig. 2. Table 2 shows the parameters derived from ultrasonic velocity measurements (based on values at 90 K), which have been corrected for transducer effect [18] and porosity [19].

The polycrystalline material can be treated as an isotropic elastic medium having two independent elastic stiffness modulus i.e. longitudinal modulus $C_L = \rho v_l^2$, shear modulus $\mu = \rho v_s^2$, with ρ is mass density, v_l is longitudinal velocity and v_s is shear

velocity. $B = C_L - \frac{4}{3}\mu$ is bulk modulus, $E = \frac{9B\mu}{3B+\mu}$ is Young's modulus and θ_D the acoustic Debye temperature, can be calculated using the standard formula,

$$\theta_D = \left(\frac{h}{k}\right)\left(\frac{3N}{4\pi V}\right)^{\frac{1}{3}} v_m$$

where $\frac{3}{v_m^{\,3}} = \frac{1}{v_l^{\,3}} + \frac{2}{v_s^{\,3}}$,

h is the Planck's constant, k is the Boltzmann's constant, N is the number of mass point, V is the atomic volume and v_m is the mean sound velocity.

Figure 2(i) shows the results of temperature-dependent ultrasound velocity and attenuation measurements for x = 0.25. At around 210 K, there is a change in slope of the shear velocity curve where the decrease in velocity with increase in temperature is much faster. This coincide with a peak in attenuation at ~230 K. The overall changes in velocity from 80 to 240 K is about 6 %, with the anomalous region accounts for 4 % changes in velocity (Δv). For longitudinal wave propagation measured between 80 to 300 K, a stiffening region between 210 to 260 K was observed. This anomalous behaviour is accompanied by a sudden increase in attenuation which peaked at two temperature within the hardening region. A small kink in velocity was also observed at 240 K. Total velocity changes from 80 to 300 K is 8 % with the anomalous region making up about 6 % of Δv. Velocity anomalies observed in both shear and longitudinal propagation are clearly related with the transition at T_c, as it occurred just below T_{IM} (260 K). Similar effect of lattice hardening below T_c has been reported before [12,14].

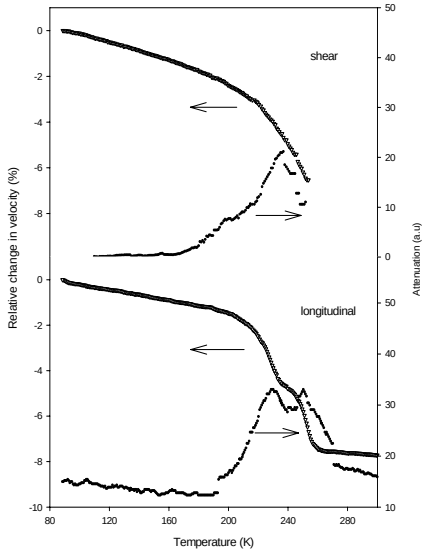

(i)

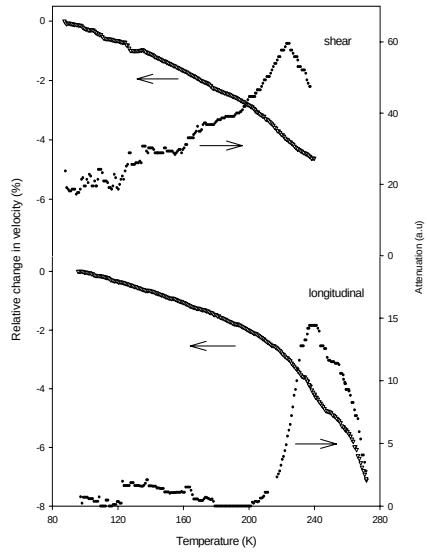

(ii)

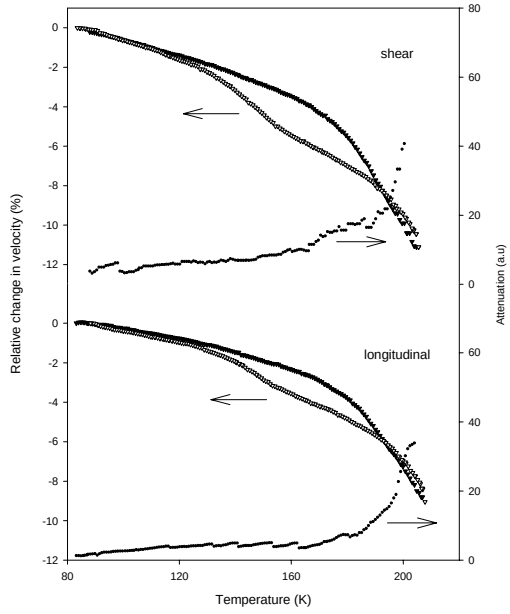

(iii)

FIGURE 2 : Temperature-dependent longitudinal and shear velocities with their attenuation for $La_{1-x}Ca_xMnO_3$ with (i) $x = 0.25$, (ii) $x = 0.33$, and (iii) $x = 0.45$

Figure 2(ii) shows results of ultrasound measurements for x = 0.33 sample. There is a slight deviation in shear velocity behaviour at around 210 K where the Δv increased. This anomalous behavior is followed by an increase in attenuation with an attenuation maxima at around 230 K. Similar trend, as in the shear mode and also observed in the ultrasonic response for x = 0.25 sample, an anomaly in longitudinal velocity curve is signified by an attenuation peak. The longitudinal velocity develops into a hardening region at around 220 K followed with an attenuation maxima at 240 K. A kink was observed at around 250 K. As with the previous samples, the attenuation and velocity anomalies for both shear and longitudinal propagation in this sample must also be related to the transition at T_c, as T_{IM} for this sample is 240 K.

For x = 0.45 sample, the striking feature is that of a large velocity hysteresis between 130 to 190 K during heating and cooling observed in both shear and longitudinal propagations (Figure 2(iii)). Change in slopes were observed at 150 K during cooling and around 180 K during warming for both modes. During cooling, the change in slope at 150 K is due to hardening tendency as the temperature decrease. During warming, the anomalous curve at around 180 K is related to a sudden increase in Δv as the temperature increase. Shear and longitudinal mode showed an almost identical sound velocity and attenuation responses. However, a smaller hysteresis occurred in the longitudinal mode. This led to a smaller velocity changes (80 to 210 K) of ~9 % in the longitudinal mode compared with 11 % in the shear mode. The percent change in sound velocity is much larger in these CMR materials compared to the high temperature superconducting cuprates for the same temperature range, for example [20]. For both modes, the attenuation showed a sudden increase at around 180 K as the temperature increase.

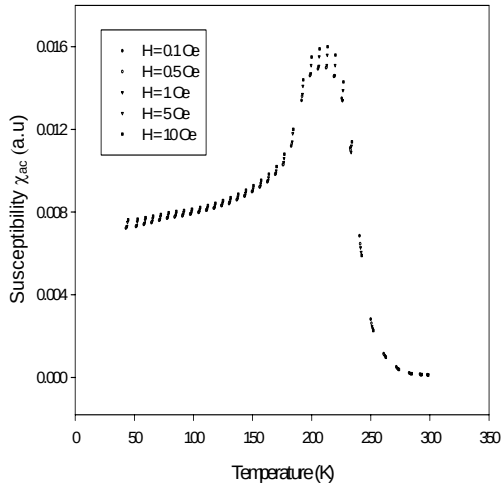

FIGURE 3 : Temperature-dependent a.c. susceptibility for $La_{0.55}Ca_{0.45}MnO_3$

Studies on this class of manganates found that for doping region near x = 0.5, the low-temperature ground state is inhomogeneous, with the double exchange, charge ordering and antiferromagnetic superexchange interactions competing against one another [16]. In an investigation by Schiffer et al. [21] on the properties of $La_{1-x}Ca_xMnO_3$

across the full range of doping within a broad temperature range, it was observed that at doping region near $x = 0.5$, the ground state changes from conducting FM to insulating AFM. This led to a first order AFM transition at $x \sim 0.50$ with large supercooling and strongly hysteretic behavior in resistivity ρ. Measurements on this compound at $x = 0.47$ doping, revealed a large thermal hysteresis in susceptibility and resistivity between 100 to 200 K [16]. These results were attributed to inhomogeneous low-temperature ground state, with conducting ferromagnetic regions coexisting with regions of charge ordering. In this work, resistivity measurement on $x = 0.45$ showed a strikingly similar behaviour with a large thermal hysteresis observed between 90 to 190 K. Results from shear and longitudinal ultrasound velocity measurements further lend support to the supposition that a similar phenomena was involved. To verify this matter, susceptibility test was performed on the sample. Result from a.c. susceptibility measurement (Figure 3) showed that at 260 K the sample undergone a ferromagnetic transition. At ~180 K a decrease in susceptibility was observed. This result is almost similar to the susceptibility result for $x = 0.47$ sample [16] discussed earlier. This allowed us to conclude that the hysteresis observed in the resistivity, the longitudinal and shear velocity measurements resulted from competition between ferromagnetic state and charge-ordered state.

Lattice hardening has been associated with a charge-ordering transition. Ramirez et al. [14] reported a large increase in sound velocity (>10 %) below T_c in $x = 0.63$ sample where the charge-ordering temperature is maximum. In this measurement, the lattice-hardening observed in both shear and longitudinal mode below 150 K during cooling could be related to the charge-ordering transition. The hardening region between 190 K to above 200 K followed by a sudden increase in attenuation in both mode of propagation, were related to the transition from higher temperature-state to a lower temperature-state. The establishment of an antiferromagnet phase brings about an anisotropic structural distortion, which is related to cooperative Jahn-Teller distortion [22]. This effect could be the reason for the smaller size of hysteresis in the longitudinal than in shear mode.

In conclusion, sound velocity and ultrasonic attenuation measurements within temperature range of 80 to 300 K have been performed on $La_{1-x}Ca_xMnO_3$ for CMR doping concentration of $x = 0.25$, 0.33 and 0.45. The elastic properties and the acoustic Debye temperature θ_D are presented. The Debye temperature is highest for the $x = 0.33$ void-free ($\theta_D = 555$ K) and non-void free ($\theta_D = 497$ K) sample. This is consistent with values reported for $La_{1-x}Sr_xMnO_3$ material obtained from heat capacity measurements [23].

For $x = 0.25$ and 0.33 samples, a huge lattice hardening observed below T_c in both longitudinal and shear propagation implies of strong electron-phonon coupling. In all cases, the hardenings were followed with a peak in attenuation. Previous theoretical studies predict a decrease in phonon damping parameter below T_c [5] which agree with results from our attenuation measurements. The phonon hardening was explained as due to the change in electron screening below T_c caused by the double exchange factor [24]. The phonon hardenings below T_c was justified by a theoretical prediction based on a model combining the double exchange and the lattice polaron [5,6]. For $x = 0.45$ sample, temperature-dependent resistivity and ultrasound measurements showed a strongly hysteretic behaviour attributed to co-existence of conducting ferromagnetic regions with charge-ordered regions. Smaller lattice hardenings in both shear and longitudinal modes below 150 K is said to be related to charge-ordered phase.

ACKNOWLEDGEMENTS

The author fully appreciate the helpful suggestions from Prof. Madya Dr. Mustaffa in the preparation of the samples and would like to express her thanks to Prof. Halim Shaari and Mr. Imad Hamadneh from UPM for the susceptibility measurement.

REFERENCES

[1] Zener, C. (1951). Phy. Rev. **82(3)**; 403.
[2] Millis, A.J., Littlewood, P.B., Shraiman, B.I. (1995). Phy. Rev. Lett. **74(25)**; 5144.
[3] Millis, A.J., Shraiman, B.I., Mueller, (1996). R. Phy. Rev. Lett. **77(1)**; 175.
[4] Millis, A.J., Mueller, R., Shraiman, B.I. (1996). Phy. Rev. B **54(8)**; 5404.
[5] Lee, J.D., Min, B.I. (1997). Phy. Rev. B **55(18)**; 12454.
[6] Unjong Yu, Min, B.I., Lee, J.D. (2000). Phy. Rev. B **61(1)**; 84.
[7] Roder, H., Zang, J., Bishop, A.R. (1996). Phy. Rev. Lett. **76(8)**; 1356.
[8] Verges, J.A., Martin-Mayor, V., Brey, L. (2002). cond-mat/0109127.
[9] Guo-Meng Zhao, Conder, K., Keller, H., Müller, K.A. (1996). Nature **381**; 676.
[10] Billinge, S.J.L., DiFrancesco, R.G., Kwei, G.H., Neumeier, J.J., Thompson, J.D. (1996). Phy. Rev. Lett. **77(4)**; 715.
[11] Shengelaya, A., Guo-meng Zhao, Keller, H., Müller, K.A. (1996). Phy. Rev. Lett. **77(26)**; 5296.
[12] Kim, K.H., Gu, J.Y., Choi, H.S., Park, G.W., Noh, T.W. (1996). Phy. Rev. Lett. **77(9)**; 1877.
[13] Fujishiro, H., Ikebe, M., Konno, Y., Fukase, T. J. (1997). Phy. Soc. Jpn. **66(12)**; 3703.
[14] Ramirez, A.P., Schiffer, P., Cheong, S.-W., Chen, C.H., Bao, W., Palstra, T.T.M., Gammel, P.L., Bishop, D.J., Zegarski, B. (1996). Phy. Rev. Lett. **76(17)**; 3188.
[15] Radaelli, P.G., Cox, D.E., Marezio, M., Cheong, S.-W., Schiffer, P.E., Ramirez, A.P. (1995). Phy. Rev. Lett. **75(24)**; 4488.
[16] Ibarra, M.R., Teresa, J.M.D. (1998). Eds. Rao, C.N.R., Raveau, B. Colossal Magnetoresistance, Charge Ordering and Related Properties of Manganese Oxides; pg. 83-155. World Scientific, Singapore.
[17] Mahesh, R., Mahendiran, R., Raychaudhuri, A.K., Rao, C.N.R. (1996). Appl. Phys. Lett. **68(16)**; 2291.
[18] Kittinger, E. (1977). Ultrasonics **15**; 30.
[19] Levy, M., Xu, M.F., Sarma, B.K., Sun, K.J. (1992). Ultrasonic propagation in sintered high-T_c superconductor. Eds. Levy, M. Physical Acoustics (XX) Ultrasonics of High-T_c and other Unconventional Superconductors; pg. 237-298. Academic Press, Inc., London.
[20] Yahya, A.K. Abd-Shukor, R. (1998). Supercond. Sci. Technol. **11(2**); 173.
[21] Schiffer, P., Ramirez, A.P., Bao, W., Cheong, S.-W. (1995). Phy. Rev. Lett. **75(18)**; 3336.
[22] Radaelli, P.G., Cox, D.E., Marezio, M., Cheong, S.-W. (1997). Phy. Rev. B **55(5)**; 3015.
[23] Okuda, T., Asamitsu, A., Tomioka, Y., Kimura, T., Taguchi, Y., Tokura, Y. (1998). Phy. Rev. Lett. **81**; 3203.
[24] Min, B.I., Lee, J.D. (1997). Physica B **230-232**; 506.